The intracellular lifestyle of an archaeal symbiont

Joshua N. Hamm[1, 2+], Yan Liao[3+], Andriko von Kügelgen[4, 5], Nina Dombrowski[2], Evan Landers[1], Christopher Brownlee[6, 7], Emma M. V. Johansson[6], Renee M. Whan[8], Matthew A. B. Baker[1], Buzz Baum[9], Tanmay A. M. Bharat[4, 5], Iain G. Duggin[3], Anja Spang[2, 10] and Ricardo Cavicchioli[1*]

[1] School of Biotechnology and Biomolecular Sciences, UNSW Sydney, Sydney, NSW 2052, Australia. [2] Royal Netherlands Institute for Sea Research, Department of Marine Microbiology and Biogeochemistry, P.O. Box 59, NL-1790 AB Den Burg, The Netherlands. [3] Australian institute for Microbiology and Infection, University of Technology Sydney, Ultimo, NSW 2007, Australia. [4] Structural Studies Division, MRC Laboratory of Molecular Biology, Francis Crick Avenue, Cambridge CB2 0QH, United Kingdom [5] Sir William Dunn School of Pathology, University of Oxford, Oxford OX1 3RE, United Kingdom. [6] Biological Resources Imaging Laboratory, Mark Wainwright Analytical Centre, University of New South Wales, Sydney, NSW 2052, Australia. [7] Fluorescence Analysis Facility, Molecular Horizons, University of Wollongong, Keiraville, NSW 2522, Australia. [8] Katharina Gaus Light Microscopy Facility, Mark Wainwright Analytical Centre, The University of New South Wales, Sydney, NSW 2052, Australia. [9]Cell Biology Division, MRC Laboratory of Molecular Biology, Francis Crick Avenue, Cambridge CB2 0QH, United Kingdom. [10]Department of Evolutionary & Population Biology, Institute for Biodiversity and Ecosystem Dynamics (IBED), University of Amsterdam, Amsterdam, The Netherlands. [+]These authors contributed equally to this work.

[*]Correspondence: R Cavicchioli, School of Biotechnology and Biomolecular Sciences, UNSW Sydney, Sydney, NSW 2052, Australia. E-mail. r.cavicchioli@unsw.edu.au

SUMMARY

DPANN *Archaea* are a diverse archaeal clade characterised by small cells and reduced genomes. To date, all cultivated DPANN *Archaea* are ectosymbionts that require direct cell-cell interactions with a host archaeal species for proliferation. However, the dynamics of DPANN – host interactions and the impacts of these interactions on host species are poorly understood. We show that the lifestyle of one DPANN archaeon (*Candidatus* Nanohaloarchaeum antarcticus) involves a cycle of attachment to host cells, invasion of the host cell cytoplasm, and subsequent lysis of the host cell. This is the first reported instance of such a predatory lifestyle amongst *Archaea* and indicates DPANN *Archaea* may be important players in microbial food webs across the biosphere. The internalisation of a symbiont cell within an archaeal host cell in the absence of phagocytotic machinery is relevant for models on the origin of the eukaryotic cell.

INTRODUCTION

The eukaryotic cell is thought to have originated through symbiosis between an archaeal host and a bacterial partner[1-3]. However, *Archaea* are not known to internalise within other archaeal cells or to be hosts of intracellular symbionts. Most known cellular endosymbionts are *Bacteria* that reside within eukaryotic cells[4]. The only known exceptions are certain methanogenic archaeal protist endosymbionts and bacterial endosymbionts of other *Bacteria*[5-7].

DPANN *Archaea* are an extremely diverse and mostly ectosymbiotic archaeal clade[8-13], but the processes by which DPANN cells associate with their hosts and proliferate are poorly understood[14]. Initially comprised of the phyla Diapherotrites, Parvarchaeota, Aenigmarchaeota, Nanoarchaeota, Nanohaloarchaeota (after which it was named), the DPANN superphylum now also includes the Woesearchaeota, Huberarchaeota, Pacearchaeota, Mamarchaeota, Micrarchaeota, and the recently identified Undinarchaeota[15, 16]. DPANN *Archaea* have been identified in a diverse range of environments including acidic hot springs[9], deep-sea sediment[10], acid mine drainage[11], microbial

mats[10], the human microbiome[13], aquifers[14] and marine waters[16, 17], as well as Antarctic lakes[8] and hypersaline systems harbouring Nanohaloarchaeota[12]. To date, all successfully cultivated DPANN *Archaea* are symbionts, requiring direct cell-cell interactions with another archaeon for proliferation[14]. Cultivation of DPANN has proven difficult, with only three lineages represented in laboratory co-cultures: the Nanoarchaeota[9, 18, 19], the Micrarchaeota[20, 21], and the Nanohaloarchaeota[8, 22].

The ectoparasitic interactions between *Ignicoccus hospitalis* and *Nanoarchaeum equitans* (the best characterised DPANN-host system) appears to involve membrane fusion between *N. equitans* and *I. hospitalis* generating a channel that connects the cytoplasms of both organisms[23]. 'Cytoplasmic bridges' have been observed between other DPANN and their hosts, and are thought to function in nutrient transfer[8, 24, 25]. However, the proteins forming or catalysing the formation of these structures are unknown[25]. Moreover, many DPANN appear to engage in interactions without forming such structures[21, 22, 26], and the mechanism by which they acquire nutrients is unclear. Furthermore, the process of cell proliferation during cultivation is poorly understood with some DPANN (*e.g.* Nanoarchaeota) remaining predominantly associated with their hosts[9], while members of other lineages (*e.g.* Nanohaloarchaeota) produce large quantities of disassociated cells[8, 25]. Thus, much remains to be learned about how DPANN attach, proliferate and detach.

Recently, the Antarctic DPANN archaeon, *Candidatus* Nanohaloarchaeum antarcticus was discovered to require the haloarchaeon *Halorubrum lacusprofundi* for growth[8]. Here we report the results of live fluorescence, cryogenic correlative light and electron microscopy, and tomography demonstrating that *Ca.* Nha. antarcticus cells bind to *Hrr. lacusprofundi* cells, fully internalise within the host cytoplasm, and subsequently trigger lysis of the host. The endoparasitic lifestyle of *Ca.* Nha. antarcticus indicates that DPANN archaea may play important roles in microbial food webs. Furthermore, the internalisation of one archaeal species within another archaeal species in the absence of phagocytosis is relevant for the assessment of models on the origin of the eukaryotic cell.

RESULTS AND DISCUSSION

Ca. Nha. antarcticus has an intracellular lifestyle

Ca. Nanohaloarchaeum antarcticus – *Halorubrum lacusprofundi* offer an ideal system for studying archaeal symbiosis, since enrichment cultures can be used to produce large numbers of nanohaloarchaeal cells (so that they make up ~50% of total cells in a co-culture at ~10^8 cells mL^{-1}), which can then be isolated and used to re-infect pure populations of host cells[8]. To investigate how *Ca.* Nha antarcticus proliferates, we used MitoTracker fluorescent dyes[26] as vital cell stains to identify and track live interactions between *Ca.* Nha. antarcticus and *Hrr. lacusprofundi* strain R1S1[27] with fluorescence and electron microscopy to investigate morphological features.

Ca. Nha. antarcticus cells purified using either fluorescence-activated cell sorting (FACS) or filtration were fluorescently stained with MitoTracker DeepRed and washed. Labelled cells were then incubated with MitoTracker Orange labelled *Hrr. lacusprofundi* R1S1 cells at a ratio of 1:1. Live co-cultures were then immobilized and cultured on an agarose gel pad or in a microfluidic flow chamber and imaged using time-lapse fluorescence microscopy, 3D laser scanning confocal microscopy, and 4D (3D time-lapse) live cell imaging. These Mitotracker dyes have been shown to be retained by haloarchaeal cells, including *Halorubrum* species, and do not affect cell growth rates[26]; as also shown here with *Hrr. lacusprofundi* (Fig. S4, S9 and S11).

A total of 163 *Hrr. lacusprofundi* cells (stained with Mitotracker Orange) were analysed in detail over the course of multiple incubations. Of these, 132 (81%) were observed with one or more *Ca.* Nha. antarcticus cell(s) attached at the first timepoint imaged (0 h), indicating that attachment predominately occurred during the initial incubation period (≤ 1 h) prior to commencement of time-lapse imaging. Over time, *Ca.* Nha. antarcticus cells appeared to progress from the exterior to the interior of *Hrr. lacusprofundi* cells (Fig. 1, S1). Confocal imaging with 3D-orthogonal projection after 10 h incubation clearly showed *Ca.* Nha. antarcticus cells had internalised within *Hrr. lacusprofundi* (Fig. 1b, S2). Internalisation typically took several hours but the exact duration varied between different observed interactions (Fig. 1, S1).

After invasion, the total area occupied by the *Ca.* Nha. antarcticus dye within the bounds of the *Hrr. lacusprofundi* cell expanded over time, implying that *Ca.* Nha. antarcticus cells grew within the host (Fig. 1a, S1, and S3). Following continued incubation, 27% (36/132) of the *Hrr. lacusprofundi* cells that were observed with attached *Ca.* Nha. antarcticus cell(s) lysed, along with 22% (36/163) of total *Hrr. lacusprofundi* cells in co-cultures (Fig. 1a, S1, 3). Note that no lysis was observed over periods of up to 70 h in control samples of pure host cells (Fig. 1a, S1, S3, and S4). Upon lysis, the dye used to label host cells in co-cultures dissipated completely, whereas labelled *Ca.* Nha. antarcticus cells remained apparently unaffected (e.g., Fig. 1a, compare 21 h and 22 h). The process of lysis occurred relatively rapidly and was complete within the 30 min time window separating imaging acquisitions.

To further investigate whether migration of the *Ca.* Nha. antarcticus cells into the *Hrr. lacusprofundi* cells corresponded to complete internalisation in live cells, a lectin cell surface stain (Concanavalin A conjugated with Alexa Fluor 350 (ConA-AF350)) and a live-cell-impermeable stain (RedDot 2) were used to label surface bound nanohaloarchaeal cells and to assess loss of host cell membrane integrity, respectively. As expected, ConA-AF350 added to co-cultures labelled *Ca.* Nha. antarcticus cells that were attached to the surface of *Hrr. lacusprofundi* (Fig. 2a, S5). By contrast, when ConA-AF350 was added to co-cultures at later timepoints (6h), many *Ca.* Nha. antarcticus cells stained negative for ConA-AF350 (Fig. 2b, S6), suggesting they had invaded their host. The absence of RedDot 2 staining indicated that these host cells had remained intact during the internalisation process (Fig. 2b, S6). As expected, host cells that were inferred to have lysed via the loss of MitoTracker Orange signal stained positive for Reddot 2 (Fig. 2c, S6). Over the course of 0 – 6 h incubations the proportion of *Hrr. lacusprofundi* lysis events associated with *Ca.* Nha. antarcticus cells increased from ~23% to ~80% while the proportion of nanohaloarchaeal cells attached to a host cell also increased from ~6% to ~41% (Fig. 2d and e, Table S2). Throughout, *Ca.* Nha. antarcticus cells associated with lysed *Hrr. lacusprofundi* cells labelled positive for both MitoTracker and Concanavalin A stains (Fig. 2c, S7).

To complement this analysis, similar experiments were performed using continuous liquid flow culture (in a microfluidics system) to assess the interactions of immobilised, MitoTracker-stained *Hrr. lacusprofundi* R1S1 cells (0.7 – 1.1 µm trap height) with MitoTracker-stained, FACS-purified, *Ca.* Nha. antarcticus cells (Fig. S3, Supplementary Video 1). As with the agarose pad experiments, *Ca.* Nha. antarcticus cell(s) were observed attaching to *Hrr. lacusprofundi* cells at the time of first imaging. Again, over a 2 – 23 h time-period, decreased signal intensity and increased area were observed for the internalised *Ca.* Nha. antarcticus cells that were suggestive of proliferation of *Ca.* Nha. antarcticus within their host (Fig. S3). During the time course, 720 *Hrr. lacusprofundi* cells lysed (52%), whereas no lysis occurred in the uninfected control (1360 cells) (Fig. S3 and S9, Table S1). Taken together, both the agarose pad and microfluidic experiments demonstrate that *Ca.* Nha. antarcticus cells induce the lysis of their hosts (11 – 52% of total *Hrr. lacusprofundi* cells were lysed versus 0% in the control, Table S1).

Experiments were also performed to investigate the effect of *Ca.* Nha. antarcticus on the cell morphology of *Hrr. lacusprofundi*, which includes rods and cocci (Fig. S9, Table S1 and ref. 28, 29). After co-incubation with *Ca.* Nha. antarcticus, 58% of 72 (agarose pad) rod-shaped *Hrr. lacusprofundi* cells had changed to a more rounded shape (Fig. S1 and S3), compared to 1.7% of control *Hrr. lacusprofundi* cells (Fig. S9, Table S1). Note that similar results were seen with the microfluidics experiments (Fig. S9, Table S1). These results suggest that the association of the two species profoundly impacts the cell biology of the host. To determine how, Cryo-CLEM (cryo-correlated light and electron microscopy) was performed to obtain high-resolution images of the fluorescently labelled cells (Fig. 1c, S12). Samples were prepared as for live fluorescence imaging, with the stained *Ca.* Nha. antarcticus and *Hrr. lacusprofundi* cells incubated together for 20 h to enable attachment and invasion. Numerous *Hrr. lacusprofundi* cells were observed that also appeared co-labelled for the MitoTracker DeepRed used to stain *Ca.* Nha. antarcticus. This included examples where DeepRed fluorescence was confined to discrete regions of the host cell as well as ones in which the fluorescent signal was present throughout the host cell (Fig. 1c, S12). In all observed examples

where *Hrr. lacusprofundi* cells were co-stained for the *Ca.* Nha. antarcticus dye, the host cell appeared intact with no obvious disruptions to its cell membrane. This suggests that the initial association, while leading to a change in shape and internalisation, does so without yet causing host cell lysis.

Structural features of the *Ca.* Nha. antarcticus symbiosis

To investigate structural features of the interactions and apparent internalisation in greater detail, higher quality three-dimensional images of *Hrr. lacusprofundi* and *Ca.* Nha. antarcticus cells were acquired in both pure samples and co-cultures using cryo-electron tomography (cryo-ET). In pure *Ca.* Nha. antarcticus samples, bulges within the membrane and cytoplasmic structures were observed in *Ca.* Nha. antarcticus cells (Fig. S13). It is possible that the cytoplasmic structures in *Ca.* Nha. antarcticus are polyhydroxyalkanoate-like (PHA-like) granules which have previously been identified in *Hrr. lacusprofundi*[30] and may be acquired from the host during interactions. The structures embedded within the *Ca.* Nha. antarcticus membrane resemble lipid droplets[31] and were also observed in the membranes of *Hrr. lacusprofundi* cells interacting with *Ca.* Nha. antarcticus cells (Fig. 3d, S14). Interestingly, these were not observed in the membranes of uninfected *Hrr. lacusprofundi* cells (Fig. S15), implying that the Nanohaloarchaeota play a role in inducing the formation of these structures. This is potentially significant as *Ca.* Nha. antarcticus lacks identifiable genes for both lipid biosynthesis and metabolism[8] and therefore has to acquire lipids from the host to survive.

Strikingly, internal membrane-bound structures were observed in several *Hrr. lacusprofundi* cells incubated with *Ca.* Nha. antarcticus and imaged by cryo-ET (Fig. 3, S16). In some cases, these appeared in intact cells (Fig. 3a – c, S16c - d) – consistent with the idea that a population of *Ca.* Nha. enters *Hrr. lacusprofundi* cells without inducing their lysis. In addition, internal structures were seen in cells that appeared damaged (Fig. S16a – b) or to have a disrupted bounding membrane (Fig. 3d – f). In general, the internalised structures proved highly radiation sensitive (Fig. S16), limiting the resolution of the images that could be obtained. However, in many instances, the membrane-bound

structures seen in co-cultures had a surface that exhibited a characteristic repeating pattern[25, 32] consistent with this being the intact S-layer of an internalised *Ca.* Nha. antarcticus cell (Fig. 3b). Archaea and bacteria are known to possess several mechanisms to prevent S-layer proteins assembling in the cytoplasm[33-35], thus these S-layers in the cytoplasm are a further strong indication of an internalised cell. While these structures were only seen in co-cultures, high-contrast granules that resemble calcium-phosphate granules[36] were observed in *Hrr. lacusprofundi* cells from both pure cultures and co-cultures (Fig 3, S14 – 16).

We also used Cryo-ET to examine the contact sites between *Ca.* Nha. antarcticus and *Hrr. lacusprofundi* cells prior to invasion (Fig. S14). In some cases, these images suggested fusion of the two cells' membranes and the opening of a cytoplasmic channel – similar to the structure of the interaction interface previously reported for *N. equitans* and *I. hospitalis* cells[23]. In these cases, the S-layers of both organisms appear to be discontinuous at the interaction site (Fig. S14). In all cases, the interaction site was limited to a region of ~15 – 20 nm in width, despite the close physical association of the two cells. By Cryo-TEM we also observed a single case of a cytoplasmic bridge extending outwards from a *Ca.* Nha. antarcticus cell (Fig. S17), resembling the structure previously described connecting *Ca.* Nha. antarcticus and *Hrr. lacusprofundi* cells based upon FISH and TEM[8]. This cytoplasmic bridge structure shows no discernible barrier between the cytoplasm of *Ca.* Nha. antarcticus and the bridge contents, suggesting that the structure may enable direct cytoplasmic transfer, as has been suggested for other DPANN[24]. However, the host cell to which the bridge extends was not clearly visible and the ultrastructure of the host associated region of the bridge has not been elucidated.

Evolutionary and ecological implications

Predatory lifestyles involving invasion of host cells and proliferation within are characteristic of viruses and some bacterial predators, most notably *Bdellovibrio bacteriovorus*[37]. However, the predatory lifestyle of *Ca.* Nha. antarcticus in co-culture with *Hrr. lacusprofundi* is the first observed

instance of such a lifestyle occurring amongst *Archaea*[14]. In contrast to *B. bacteriovorus,* which invades the periplasm[37], here we provide evidence that *Ca.* Nha. antarcticus enters the host cytoplasm. Due to differences of the cell envelope structures of the host species, *Ca.* Nha. antarcticus and *B. bacteriovorus* both accomplish internalization by crossing a single lipid bilayer without destabilising the host cell. After internalization, *B. bacteriovorus* proliferates within the host's periplasm[37], and our data suggests that *Ca.* Nha. antarcticus proliferates within the host's cytoplasm (the *Ca.* Nha. antarcticus lifestyle is conceptualised in Fig. 4). The precise mechanisms and regulation of the *Ca.* Nha. antarcticus proliferation process remain to be determined including whether cell division can occur following lysis of the host and release of internalised nanohaloarchaeal cells.

It is unclear how widespread this parasitic lifestyle may be amongst DPANN *Archaea* as the majority of DPANN species are uncultivated[14] and the environmental factors that influence growth of DPANN remain enigmatic. However, the characteristics we describe in this paper illustrate the potential capacity of certain DPANN *Archaea* to contribute to nutrient cycling through lysis of host cells, similar to viral predation in the top-down control of the food web in Antarctic aquatic systems[38]. In this way, *Ca.* Nha antarcticus is likely to contribute to the recycling of nutrients in the three haloarchaeal-dominated, hypersaline lakes that it is known to colonise[8]. Furthermore, it has been suggested that DPANN *Archaea* may associate not only with other *Archaea* but also with *Eukarya* and *Bacteria*[14, 15, 39]. The capacity for some of the diverse types of DPANN *Archaea*[8-17] to behave in a predatory manner similar to viruses could have broad implications for microbial food web dynamics across the globe and may necessitate a re-evaluation of their functional importance and ecological roles.

A range of symbiogenetic models for the evolution of *Eukarya* have been proposed (reviewed in ref. 3). In particular, recent discoveries have provided increasing support for the hypothesis that *Eukarya* emerged through a symbiosis between *Archaea* and *Bacteria*[1-3, 40]. While an archaeal lineage related to Asgard *Archaea* likely represented the host cell, mitochondria and chloroplasts derived

from internalised Alphaproteobacteria and Cyanobacteria, respectively. However, a mechanistic understanding of the interactions that could have enabled such intricate interactions is lacking because *Archaea* have so far not been found to be able to host endosymbionts nor to internalise within other archaeal or bacterial cells. By demonstrating that the archaeal cytoplasm is susceptible to invasion and capable of fulfilling the life cycle of a symbiont, our findings show that it is possible for a symbiont to enter an archaeal host in the absence of a phagocytotic pathway[2-4]. By extension, it is possible that a similar process may have facilitated the generation of eukaryotic organelles. In particular, the internalisation of *Ca.* Nha. antarcticus within *Hrr. lacusprofundi* does not involve acquisition of an additional lipid bilayer surrounding the symbiont cell, a feature shared by modern mitochondria which retain the dual lipid bilayer structure of their free-living ancestors. Internalisation via phagocytosis would initially yield a three lipid bilayer envelope structure which is not found in extant endosymbionts. Our findings provide precedent for alternative systems of symbiont internalisation active in extant *Archaea* that yield cell envelopes consistent with those of eukaryotic organelles. The systems enabling internalisation in the archaeal ancestor of eukaryotes are likely analogous, rather than homologous, to those in *Ca.* Nha. antarcticus and possibly other DPANN *Archaea*. Precisely how the cells enter the host remains an important question for the future. However, it is clear that gaining a detailed understanding of the interaction between *Ca.* Nha. antarcticus – *Hrr. lacusprofundi* in co-cultures and other similar symbiotic systems is likely to inform our understanding of the cell-cell interactions that underpin eukaryogenesis.

METHODS

Production of nanohaloarchaeal cells

Purified *Ca.* Nha. antarcticus cells were sourced from an enrichment culture (Nha-CHl) grown at 18 °C by FACS as previously described[8] or through filtration. To acquire *Ca.* Nha. antarcticus through filtration 10 mL of the Nha-CHl culture was first filtered three times through a 0.8 µm pore size cellulose acetate syringe filter and then subsequently filtered five times through a 0.22 µm pore size

cellulose acetate syringe filter. The resulting filtrate was centrifuged at 20,000 *g* for 10 min and the cell pellet was resuspended in 1 mL of fresh DBCM2[8]. To confirm purity of filtered cells, aliquots were spot plated on DBCM2 agar and incubated for 2 months at 30 °C. Absence of growth indicated filtration had successfully removed *Hrr. lacusprofundi* cells from the sample. *Hrr. lacusprofundi* strain R1S1[41] cells were grown as previously described for strain ACAM34[8], and after two weeks growth, incubated with FACS-purified *Ca.* Nha. antarcticus cells.

Live fluorescence microscopy

MitoTracker dye (1:1000 dilution; 1 µM final centration) was added to 500 µL of *Ca. Nha. antarcticus* sorted cells (~ 2 x 10^7 mL^{-1}; MitoTracker Deep Red FM) or *Hrr. lacusprofundi* cells (~ 3 x 10^8 mL^{-1}; MitoTracker Orange CMTMRos)[26]. Cells were maintained at 30°C with static incubation for 1 h. The dye was washed out three times with fresh DBCM2 media[8] via centrifugation after staining and resuspended in 50 µL (*Ca. Nha. antarcticus* cells) or 250 µL (*Hrr. lacusprofundi*) of DBCM2 media. Resuspended *Hrr. lacusprofundi* (2 µl) and *Ca. Nha. antarcticus* (4 µL) cells were mixed prior to use. For live-cell fluorescent microscopy imaging, 3 µL of mixed cells was placed on a ~1 mm thick agarose pad (0.3% w/v agarose and containing the full media requirements for DBCM2 media), that had been prepared on a 8 mm diameter #1.5 circular glass coverslip (World Precision Instruments, Inc). The coverslip-pad-cell sample assembly was placed inverted onto the base of a 35 mm #1.5 FluoroDish (WPI)[42]. The pre-warmed (30°C) liquid DBCM2 medium (4 mL) was gently applied to cover the pad assembly in the FluoroDish. The lid was applied to avoid evaporation and the dish was incubated on the microscope stage (at 30°C) for imaging. The initial stages of microscope setup for obtaining images of multiple, individual cells took ~ 1 h, meaning that cells had the opportunity to interact prior to the initiation (t_0) of the time course. Time-lapse fluorescence imaging was performed at 30°C on a Nikon Ti-E-Perfect Focus microscope with DS-Qi2 camera and a × 100 Oil Plan NA 1.45 objective using a TRITC filter (Ex: 535/36 nm; Em: 590/34 nm) for the MitoTracker Orange fluorescence signal, and a Cy5 filter (Ex: 645/30 nm; Em: 660/40 nm) for the MitoTracker

Deep Red fluorescence signal. Z-stack imaging was performed on a confocal laser scanning Nikon A1 microscope with A1-DUG GaAsP Multi Detector Unit (hybrid 4-channel detector: 2 GaAsP PMTs + 2 normal PMTs) at 30°C using a Plan Fluor 100 × Oil objective (z-axis step 0.125 µm) with the TRITC filter (Ex: GaAsP 561 nm; Em: 595/50 nm) and Alx647 channel (Ex:PMT, 637.4 nm; Em 700/75 nm), or on a DeltaVision Elite microscope at 30°C using a 100 × Oil NA 1.4 objective (Z-axis step 0.2 µm or 0.5 µm) with the TRITC and Cy5 filters. The imaging data were processed for deconvolution and bleach correction as stated in the figure legend. The processed Z-stack data were re-constructed for 3D 'orthogonal' slice projection analyses using the Imaris software package (Bitplane AG, Zurich, Switzerland).

To determine whether migration of the *Ca.* Nha. antarcticus stain into *Hrr. lacusprofundi* R1S1 cells corresponded to internalisation or invagination, cells were stained with either MitoTracker Orange (*Hrr. lacusprofundi* R1S1) or MitoTracker Green (*Ca.* Nha. antarcticus) as described above (1 µM final concentration). Cells were then mixed and incubated at 30°C. Samples (10 µL) were taken hourly and additionally stained with Concanavalin A (Alexa Fluor 350 conjugated, 200 µg/mL) and RedDot 2 (200X solution diluted to 1X final concentration). Cells were mounted onto glass slides and imaged on a Carl Zeiss Imager M.2 microscope at room temperature with a 100× Neofluor objective using a Carl Zeiss filter sets 02 (Ex: G 365 nm; Em: LP 420 nm), 38 (Ex: BP 470/40 nm; Em: BP 525/50 nm), 00 (Ex: BP 530-585 nm; Em: LP 615 nm), and 50 (Ex: BP 640/30 nm, Em: BP 690/50 nm). To assess the effects of MitoTracker dye on cell growth, *Hrr. lacusprofundi* R1S1 cells were stained with MitoTracker Orange (1 µM final concentration) as described above. MitoTracker-stained and unstained control cells were each inoculated into 5 mL fresh DBCM2 medium in 50 mL conical tubes (three biological replicates) to an optical density (OD_{595}) of ~0.05, cultures incubated with shaking (150 RPM) at 30 ºC, duplicate aliquots dispensed daily into microtitre plates, and OD_{595} monitored using a SpectraMax 190 Microplate Reader (Molecular Devices LLC) with fresh DBCM2 medium as a blank. To assess the effects of MitoTracker dye reversal on the interactions between *Ca.* Nha. antarcticus and *Hrr. lacusprofundi*, FACS-purified *Ca.* Nha. antarcticus cells were stained with

MitoTracker Orange CMTMRos (1 µM final centration), *Hrr. lacusprofundi* R1S1 cells were stained with MitoTracker Deep Red FM (1 µM final concentration), and cell mixtures were imaged using fluorescence time-lapse microscopy as described above. Reversing the labelling with dyes yielded analogous results to prior experiments (Fig. S8). To assess the effects of cell fixation on interactions between *Ca.* Nha. antarcticus and *Hrr. lacusprofundi*, FACS-purified *Ca.* Nha. antarcticus cells (500 µL, ~ 2 x 10^7 mL^{-1}) were pelleted (5 min, 19,745 *g*) and gently resuspended in 1 mL 18% buffered salt water[43] containing 4 % (v/v) paraformaldehyde (PFA) and cells fixed by shaking (250 RPM) at room temperature overnight. The fixed cells were washed twice by centrifugation (5 min, 19,745 *g*), and the cell pellet resuspended in 500 µL DBCM2 medium. The fixed *Ca.* Nha. antarcticus cells were stained with MitoTracker Deep Red FM and incubated with *Hrr. lacusprofundi* R1S1 cells stained with MitoTracker Orange CMTMRos, and the cells imaged as described above. Pre-treatment of *Ca.* Nha. antarcticus cells with paraformaldehyde led to a reduced number of *Hrr. lacusprofundi* cells with attached *Ca.* Nha. antarcticus cells (106 of 186 imaged *Hrr. lacusprofundi* cells; 57 %) and subsequently fewer lysed *Hrr. lacusprofundi* cells (12 cells; 6.5%) (Fig. S8, Table S1). Pre-treatment of the *Hrr. lacusprofundi* cells with paraformaldehyde also resulted in a substantial reduction in the frequency of both attachment (31 of 265 imaged *Hrr. lacusprofundi* cells; 11.7%) and lysis events (no cells: 0%) (Fig. S8, Table S1). Agarose pad time-course experiments were performed by staining *Hrr. lacusprofundi* R1S1 cells with MitoTracker Orange CMTMRos and FACS-purified *Ca.* Nha. antarcticus cells with MitoTracker Deep Red FM, as described above. The mixed cultures were sampled at different time-points (0, 3, 6, 9, 12 and 24 h) and placed on a 1 % (w/v) agarose pad containing DBCM2 basal salts on a glass slide with a #1.5 glass coverslip placed on top, and cells imaged as described above.

Microfluidic time-course interactions between *Ca.* Nha. antarcticus and *Hrr. lacusprofundi* were performed using a CellASIC ONIX2 microfluidics system to immobilize and record live cells that were exposed to a constant flow of liquid. CellASIC B04A plates (EMD Millipore) were equilibrated with 1 mg mL^{-1} Bovine Serum Albumin in phosphate-buffered saline followed by DBCM2 basal salts at a

constant flow pressure of 5 psi. The mixed cell culture (*Hrr. lacusprofundi* R1S1 stained with MitoTracker Orange CMTMRos, and FACS-purified *Ca.* Nha. antarcticus cells stained with MitoTracker Deep Red FM) were loaded into the microfluidics chamber and perfused with DBCM2 medium at 0.25 psi for up to 48 h. Cells were imaged at 30 °C every hour or 30 min using a Nikon TiE2 inverted microscope fitted with a 100× oil-immersion phase-contrast NA 1.45 objective.

For display purposes, time-lapse images were prepared by using OMERO and where needed adjusted for enhancing brightness with same setting applied to the whole image series. The quantitative analysis for the attachment, lysis, morphological change events and cell area were performed by combining automated detection (in FIJI 1.52P[44] and Microbe J 5.13I[45]) and manual curation. Cell outlines were detected in MicrobeJ by phase-contrast image using the Local Default method and manually corrected where needed. Fluorescence signals were detected by 'Maxima' in Microbe J using the Foci and Basic modes (*Hrr. lacusprofundi* fluorescence: tolerance 1000, Z score 20, area > 0.5 intensity > 800; *Ca.* Nha. antarcticus fluorescence: tolerance 1000, Z-score 6, area > 0.05, intensity > 200). For quantification of interactions in experiments using MitoTracker Green and Orange, Concanavalin A, and Reddot 2, channels were subjected to auto thresholding (Moments dark stack: MitoTracker Green, MitoTracker Orange, and Reddot 2; MaxEntropy dark stack: Concanavalin A). Channels were then converted to binary masks and particles counted ("Analyze Particles...", "size=0.1-Infinity summarize in_situ"). Interactions between *Ca.* Nha. antarcticus and *Hrr. lacusprofundi* were quantified by taking overlaps between MitoTracker Green and MitoTracker Orange (ImageCalculator("AND create")) and counting particles ("Analyze Particles...", "summarize in_situ"). Association of *Ca.* Nha. antarcticus with lysis events was quantified by taking overlaps between MitoTracker Green and Reddot 2 (ImageCalculator("AND create")) and counting particles ("Analyze Particles...", "summarize in_situ").

Cryo electron microscopy and tomography

For cryo-CLEM, purified *Ca.* Nha. antarcticus and *Hrr. lacusprofundi* cells were stained as described (see **Live fluorescence microscopy**), mixed at a cell-to-cell ratio of 1:3 and incubated for a period of 20 h. Samples were screened using an Olympus BX61 microscope using cellSens v2.2 software (Olympus Corporation) in order to assess staining. Once screened, the sample was loaded onto Quantifoil carbon coated grids (R 2/2; Quantifoil Micro Tools, Jena, Germany) and cryo-fixed by plunge freezing with a Leica GP (Leica Microsystems) into liquid ethane, as previously described[46]. Grids were assembled into autogrids and imaged using a Zeiss LSM 900 upright confocal with Airyscan 2 fluorescence microscope on a Linkam CMS196 Cryo-correlative microscopy stage with a 100x NA 0.75 objective using a TRITC filter at an excitation of 561 nm for MitoTracker Orange and a Cy5 filter at an excitation of 647 nm for MitoTracker DeepRed. Images were acquired using an Axiocam 506 mono camera (Carl Zeiss AG). Autogrids were transferred for imaging on a Talos Arctica Cryo-electron microscope at 200 kV. For cryo-ET of fluorescently labelled and internalised *Ca.* Nha. antarcticus cells, tilt series were acquired at binning 2 on a Falcon 3 camera under the controls of Tomography software (ThermoFisher). For cryo-ET of the enrichment culture, biomass was loaded onto Quantifoil carbon coated grids (Quantifoil Micro Tools, Jena, Germany) and imaged on a Titan Krios (Thermo Fisher Scientific, Waltham, Massachusetts) at 300 kV. Defocus for all images was -10 µm. For cryo-ET of *Hrr. lacusprofundi* – *Ca.* Nha. antarcticus co-cultures cells were mixed as described above for fluorescence microscopy and incubated at 30°C for 17 h. Cells were then loaded onto Quantifoil holey carbon coated grids (Cu/Rh 3.5/1 200 mesh for *Hrr. lacusprofundi* cells and co-cultures and Cu/Rh 2/2 200 mesh for the pure *Ca.* Nha. antarcticus cells). Samples were cryo-fixed by plunge-freezing in liquid ethane using a Vitrobot Mark IV and stored under liquid nitrogen until imaging, as previously described[47]. Imaging was performed on a Titan Krios at 300 kV using a Bioquantum energy filter and the K3 detector (Gatan Inc.). Tilt series was collected at 2º increments between ±60º, defocus was varied from -6 to -12 µm depending on the tilt series (specified in figure legends), and a total dose of 80 e-/Å^2 was applied over the series. Tomographic reconstructions were performed using IMOD (http://bio3d.colorado.edu/imod/)[48] and tomo3D[49].

REFERENCES

1 Martijn, J., and Ettema, T.J. (2013). From archaeon to eukaryote: the evolutionary dark ages of the eukaryotic cell. Biochem Soc Trans *41*, 451-457.

2 Eme, L., Spang, A., Lombard, J., Stairs, C.W., and Ettema, T.J.G. (2018). Archaea and the origin of eukaryotes. Nat Rev Microbiol *16*, 120.

3 Lopez-Garcia, P., Eme, L., and Moreira, D. (2017). Symbiosis in eukaryotic evolution. J Theor Biol *434*, 20-33.

4 Zachar, I., and Boza, G. (2020). Endosymbiosis before eukaryotes: mitochondrial establishment in protoeukaryotes. Cell Mol Life Sci *77*, 3503-3523.

5 Kellner, S., Spang, A., Offre, P., Szollosi, G.J., Petitjean, C., and Williams, T.A. (2018). Genome size evolution in the Archaea. Emerg Top Life Sci *2*, 595-605.

6 Lind, A.E., Lewis, W.H., Spang, A., Guy, L., Embley, T.M., and Ettema, T.J.G. (2018). Genomes of two archaeal endosymbionts show convergent adaptations to an intracellular lifestyle. ISME J *12*, 2655-2667.

7 von Dohlen, C.D., Kohler, S., Alsop, S.T., and McManus, W.R. (2001). Mealybug beta-proteobacterial endosymbionts contain gamma-proteobacterial symbionts. Nature *412*, 433-436.

8 Hamm, J.N., Erdmann, S., Eloe-Fadrosh, E.A., Angeloni, A., Zhong, L., Brownlee, C., Williams, T.J., Barton, K., Carswell, S., Smith, M.A.*, et al.* (2019). Unexpected host dependency of Antarctic Nanohaloarchaeota. Proc Natl Acad Sci U S A *116*, 14661-14670.

9 Huber, H., Hohn, M.J., Rachel, R., Fuchs, T., Wimmer, V.C., and Stetter, K.O. (2002). A new phylum of Archaea represented by a nanosized hyperthermophilic symbiont. Nature *417*, 63-67.

10 Liu, X., Li, M., Castelle, C.J., Probst, A.J., Zhou, Z., Pan, J., Liu, Y., Banfield, J.F., and Gu, J.D. (2018). Insights into the ecology, evolution, and metabolism of the widespread Woesearchaeotal lineages. Microbiome *6*, 102.

11 Baker, B.J., Comolli, L.R., Dick, G.J., Hauser, L.J., Hyatt, D., Dill, B.D., Land, M.L., Verberkmoes, N.C., Hettich, R.L., and Banfield, J.F. (2010). Enigmatic, ultrasmall, uncultivated Archaea. Proc Natl Acad Sci U S A *107*, 8806-8811.

12 Narasingarao, P., Podell, S., Ugalde, J.A., Brochier-Armanet, C., Emerson, J.B., Brocks, J.J., Heidelberg, K.B., Banfield, J.F., and Allen, E.E. (2012). De novo metagenomic assembly reveals abundant novel major lineage of Archaea in hypersaline microbial communities. ISME J *6*, 81-93.

13 Koskinen, K., Pausan, M.R., Perras, A.K., Beck, M., Bang, C., Mora, M., Schilhabel, A., Schmitz, R., and Moissl-Eichinger, C. (2017). First Insights into the Diverse Human Archaeome: Specific Detection of Archaea in the Gastrointestinal Tract, Lung, and Nose and on Skin. Mbio *8*.

14 Dombrowski, N., Lee, J.H., Williams, T.A., Offre, P., and Spang, A. (2019). Genomic diversity, lifestyles and evolutionary origins of DPANN archaea. FEMS Microbiol Lett *366*.

15 Castelle, C.J., Brown, C.T., Anantharaman, K., Probst, A.J., Huang, R.H., and Banfield, J.F. (2018). Biosynthetic capacity, metabolic variety and unusual biology in the CPR and DPANN radiations. Nat Rev Microbiol *16*, 629-645.

16 Dombrowski, N., Williams, T.A., Sun, J., Woodcroft, B.J., Lee, J.H., Minh, B.Q., Rinke, C., and Spang, A. (2020). Undinarchaeota illuminate DPANN phylogeny and the impact of gene transfer on archaeal evolution. Nat Commun *11*, 3939.

17 Tully, B.J., Graham, E.D., and Heidelberg, J.F. (2018). The reconstruction of 2,631 draft metagenome-assembled genomes from the global oceans. Sci Data *5*, 170203.

18 St John, E., Liu, Y., Podar, M., Stott, M.B., Meneghin, J., Chen, Z., Lagutin, K., Mitchell, K., and Reysenbach, A.L. (2019). A new symbiotic nanoarchaeote (Candidatus Nanoclepta minutus) and its host (Zestosphaera tikiterensis gen. nov., sp. nov.) from a New Zealand hot spring. Syst Appl Microbiol *42*, 94-106.

19 Wurch, L., Giannone, R.J., Belisle, B.S., Swift, C., Utturkar, S., Hettich, R.L., Reysenbach, A.L., and Podar, M. (2016). Genomics-informed isolation and characterization of a symbiotic Nanoarchaeota system from a terrestrial geothermal environment. Nat Commun *7*, 12115.

20 Krause, S., Bremges, A., Munch, P.C., McHardy, A.C., and Gescher, J. (2017). Characterisation of a stable laboratory co-culture of acidophilic nanoorganisms. Sci Rep *7*, 3289.

21 Golyshina, O.V., Toshchakov, S.V., Makarova, K.S., Gavrilov, S.N., Korzhenkov, A.A., La Cono, V., Arcadi, E., Nechitaylo, T.Y., Ferrer, M., Kublanov, I.V.*, et al.* (2017). 'ARMAN' archaea depend on association with euryarchaeal host in culture and in situ. Nat Commun *8*, 60.

22 La Cono, V., Messina, E., Rohde, M., Arcadi, E., Ciordia, S., Crisafi, F., Denaro, R., Ferrer, M., Giuliano, L., Golyshin, P.N.*, et al.* (2020). Symbiosis between nanohaloarchaeon and haloarchaeon is based on utilization of different polysaccharides. Proc Natl Acad Sci U S A *117*, 20223-20234.

23 Heimerl, T., Flechsler, J., Pickl, C., Heinz, V., Salecker, B., Zweck, J., Wanner, G., Geimer, S., Samson, R.Y., Bell, S.D.*, et al.* (2017). A Complex Endomembrane System in the Archaeon Ignicoccus hospitalis Tapped by Nanoarchaeum equitans. Front Microbiol *8*, 1072.

24 Comolli, L.R., and Banfield, J.F. (2014). Inter-species interconnections in acid mine drainage microbial communities. Front Microbiol *5*, 367.

25 Krause, S., Gfrerer, S., von Kugelgen, A., Reuse, C., Dombrowski, N., Villanueva, L., Bunk, B., Sproer, C., Neu, T.R., Kuhlicke, U.*, et al.* (2022). The importance of biofilm formation for

cultivation of a Micrarchaeon and its interactions with its Thermoplasmatales host. Nat Commun *13*, 1735.

26 Maslov, I., Bogorodskiy, A., Mishin, A., Okhrimenko, I., Gushchin, I., Kalenov, S., Dencher, N.A., Fahlke, C., Buldt, G., Gordeliy, V.*, et al.* (2018). Efficient non-cytotoxic fluorescent staining of halophiles. Sci Rep *8*, 2549.

27 Tschitschko, B., Erdmann, S., DeMaere, M.Z., Roux, S., Panwar, P., Allen, M.A., Williams, T.J., Brazendale, S., Hancock, A.M., Eloe-Fadrosh, E.A.*, et al.* (2018). Genomic variation and biogeography of Antarctic haloarchaea. Microbiome *6*.

28 Franzmann, P.D., Stackebrandt, E., Sanderson, K., Volkman, J.K., Cameron, D.E., Stevenson, P.L., McMeekin, T.A., and Burton, H.R. (1988). Halobacterium lacusprofundi sp. nov., a Halophilic Bacterium Isolated from Deep Lake, Antarctica. Systematic and Applied Microbiology *11*, 20-27.

29 Liao, Y., Williams, T.J., Ye, J., Charlesworth, J., Burns, B.P., Poljak, A., Raftery, M.J., and Cavicchioli, R. (2016). Morphological and proteomic analysis of biofilms from the Antarctic archaeon, Halorubrum lacusprofundi. Sci Rep *6*, 37454.

30 Williams, T.J., Liao, Y., Ye, J., Kuchel, R.P., Poljak, A., Raftery, M.J., and Cavicchioli, R. (2017). Cold adaptation of the Antarctic haloarchaea Halohasta litchfieldiae and Halorubrum lacusprofundi. Environ Microbiol *19*, 2210-2227.

31 Murphy, D.J. (2012). The dynamic roles of intracellular lipid droplets: from archaea to mammals. Protoplasma *249*, 541-585.

32 von Kugelgen, A., Alva, V., and Bharat, T.A.M. (2021). Complete atomic structure of a native archaeal cell surface. Cell Rep *37*, 110052.

33 Bharat, T.A.M., von Kugelgen, A., and Alva, V. (2021). Molecular Logic of Prokaryotic Surface Layer Structures. Trends Microbiol *29*, 405-415.

34 Herdman, M., von Kugelgen, A., Kureisaite-Ciziene, D., Duman, R., El Omari, K., Garman, E.F., Kjaer, A., Kolokouris, D., Lowe, J., Wagner, A.*, et al.* (2022). High-resolution mapping of metal ions reveals principles of surface layer assembly in Caulobacter crescentus cells. Structure *30*, 215-228 e215.

35 von Kugelgen, A., Tang, H., Hardy, G.G., Kureisaite-Ciziene, D., Brun, Y.V., Stansfeld, P.J., Robinson, C.V., and Bharat, T.A.M. (2020). In Situ Structure of an Intact Lipopolysaccharide-Bound Bacterial Surface Layer. Cell *180*, 348-358 e315.

36 Strubbe-Rivera, J.O., Schrad, J.R., Pavlov, E.V., Conway, J.F., Parent, K.N., and Bazil, J.N. (2021). The mitochondrial permeability transition phenomenon elucidated by cryo-EM reveals the genuine impact of calcium overload on mitochondrial structure and function. Sci Rep *11*, 1037.

37 Chanyi, R.M., and Koval, S.F. (2014). Role of type IV pili in predation by Bdellovibrio bacteriovorus. PLoS One *9*, e113404.

38 Cavicchioli, R. (2015). Microbial ecology of Antarctic aquatic systems. Nat Rev Microbiol *13*, 691-706.

39 Reysenbach, A.L., St John, E., Meneghin, J., Flores, G.E., Podar, M., Dombrowski, N., Spang, A., L'Haridon, S., Humphris, S.E., de Ronde, C.E.J.*, et al.* (2020). Complex subsurface hydrothermal fluid mixing at a submarine arc volcano supports distinct and highly diverse microbial communities. Proc Natl Acad Sci U S A *117*, 32627-32638.

40 Spang, A., Saw, J.H., Jorgensen, S.L., Zaremba-Niedzwiedzka, K., Martijn, J., Lind, A.E., van Eijk, R., Schleper, C., Guy, L., and Ettema, T.J.G. (2015). Complex archaea that bridge the gap between prokaryotes and eukaryotes. Nature *521*, 173-179.

41 Erdmann, S., Tschitschko, B., Zhong, L., Raftery, M.J., and Cavicchioli, R. (2017). A plasmid from an Antarctic haloarchaeon uses specialized membrane vesicles to disseminate and infect plasmid-free cells. Nat Microbiol *2*, 1446-1455.

42 Duggin, I.G., Aylett, C.H., Walsh, J.C., Michie, K.A., Wang, Q., Turnbull, L., Dawson, E.M., Harry, E.J., Whitchurch, C.B., Amos, L.A.*, et al.* (2015). CetZ tubulin-like proteins control archaeal cell shape. Nature *519*, 362-365.

43 Dyall-Smith, M. (2015). The Halohandbook v7.3.

44 Schindelin, J., Arganda-Carreras, I., Frise, E., Kaynig, V., Longair, M., Pietzsch, T., Preibisch, S., Rueden, C., Saalfeld, S., Schmid, B.*, et al.* (2012). Fiji: an open-source platform for biological-image analysis. Nat Methods *9*, 676-682.

45 Ducret, A., Quardokus, E.M., and Brun, Y.V. (2016). MicrobeJ, a tool for high throughput bacterial cell detection and quantitative analysis. Nat Microbiol *1*, 16077.

46 Dubochet, J., and McDowall, A.W. (1981). Vitrification of pure water for electron microscopy. Journal of Microscopy *124*.

47 Sulkowski, N.I., Hardy, G.G., Brun, Y.V., and Bharat, T.A.M. (2019). A Multiprotein Complex Anchors Adhesive Holdfast at the Outer Membrane of Caulobacter crescentus. Journal of Bacteriology *201*, e00112-00119.

48 Mastronarde, D.N., and Held, S.R. (2017). Automated tilt series alignment and tomographic reconstruction in IMOD. J Struct Biol *197*, 102-113.

49 Agulleiro, J.I., and Fernandez, J.J. (2015). Tomo3D 2.0--exploitation of advanced vector extensions (AVX) for 3D reconstruction. J Struct Biol *189*, 147-152.

ACKNOWLEDGEMENTS

We thank Sarah Brazendale, Alice M. Hancock and expedition personnel for obtaining Antarctic samples. The live fluorescence microscopy results were obtained at UTS Microbial Imaging Facility, and we thank Chris Evenhuis, Michael Johnson, and Louise Cole for technical support. The authors acknowledge the use of the Cryo Electron Microscopy Facility through the Victor Chang Cardiac Research Institute Innovation Centre, funded by the NSW government. Electron microscopy results were obtained at the Electron Microscope Unit, within the Mark Wainwright Analytical Centre of the University of New South Wales and at the Structural Studies Division, MRC Laboratory of Molecular Biology. Cryogenic Light microscopy was performed at the Biomedical Imaging Facility within the Mark Wainwright Analytical Centre of the University of New South Wales. Fluorescence Activated Cell Sorting was performed at the Flow Cytometry Facility within the Mark Wainwright Analytical Centre of the University of New South Wales. We thank Nicholas Ariotti, Joanna Biazik, Hariprasad Venugopal, Gediminas Gervinskas, and Georg Ramm for assistance developing electron microscopy approaches. DNA sequencing of PCR products was performed at the Ramaciotti Centre for Genomics (UNSW Sydney), and computational analyses were performed on the computational cluster Katana, supported by the Faculty of Science (UNSW Sydney). This work was supported by the Australian Research Council (DP150100244 to R. C.; FT160100010 to I. G. D.), the Australian Antarctic Science program (project 4031 to R. C.), the UTS Chancellor's Postdoctoral Research Fellowship (PRO21-13161 to Y.L), the Swedish Research Council (VR starting grant 2016-03559 to A. S. and supporting J. H.), the NWO-I foundation of the Netherlands Organisation for Scientific Research (WISE fellowship to A. S.), the European Research Council (ERC) under the European Union's Horizon 2020 research and innovation programme (grant agreement ERC Starting grant No. 947317 to A. S.) as well as by the Moore–Simons Project on the Origin of the Eukaryotic Cell, Simons Foundation 735929LPI, https://doi.org/10.46714/735929LPI. (Award Number: 811944 to A. S. and supporting J. H.). T. A. M. B. would like to thank UKRI MRC (Programme MC_UP_1201/31), the Human Frontier Science Programme (Grant RGY0074/2021), the Vallee Research Foundation, the European Molecular

Biology Organization, the Leverhulme Trust and the Lister Institute for Preventative Medicine for support.

AUTHOR CONTRIBUTIONS

J. N. H., Y.L., and R. C. conceived the study. J. N. H., Y. L., E. L., C. B., and E. M. V. J. performed cultivation and purification of *Ca.* Nha. antarcticus cells. Y. L., I. G. D., J. N. H, and A. S. conducted live fluorescence microscopy. J. N. H., A. v. K, T. A. M. B, E. L, M. A. B. B., and R. M. W performed electron microscopy. J. N. H, Y. L., A. v. K, T. A. M. B, N. D., E. L., A. S., and R. C. conducted data interpretation. J. N. H, Y. L., A. v. K, T. A. M. B, N. D., E. L., A. S., and R. C. wrote the manuscript with input from all other co-authors. All authors have read and approved the manuscript submission.

COMPETING INTERESTS

The authors declare no competing financial interests and no conflict of interest.

CORRESPONDING AUTHOR

Correspondence to Ricardo Cavicchioli: r.cavicchioli@unsw.edu.au

DATA AND MATERIALS AVAILABILITY

Supplementary data are available in our repository on figshare [https://doi.org/10.6084/m9.figshare.12957092]

a

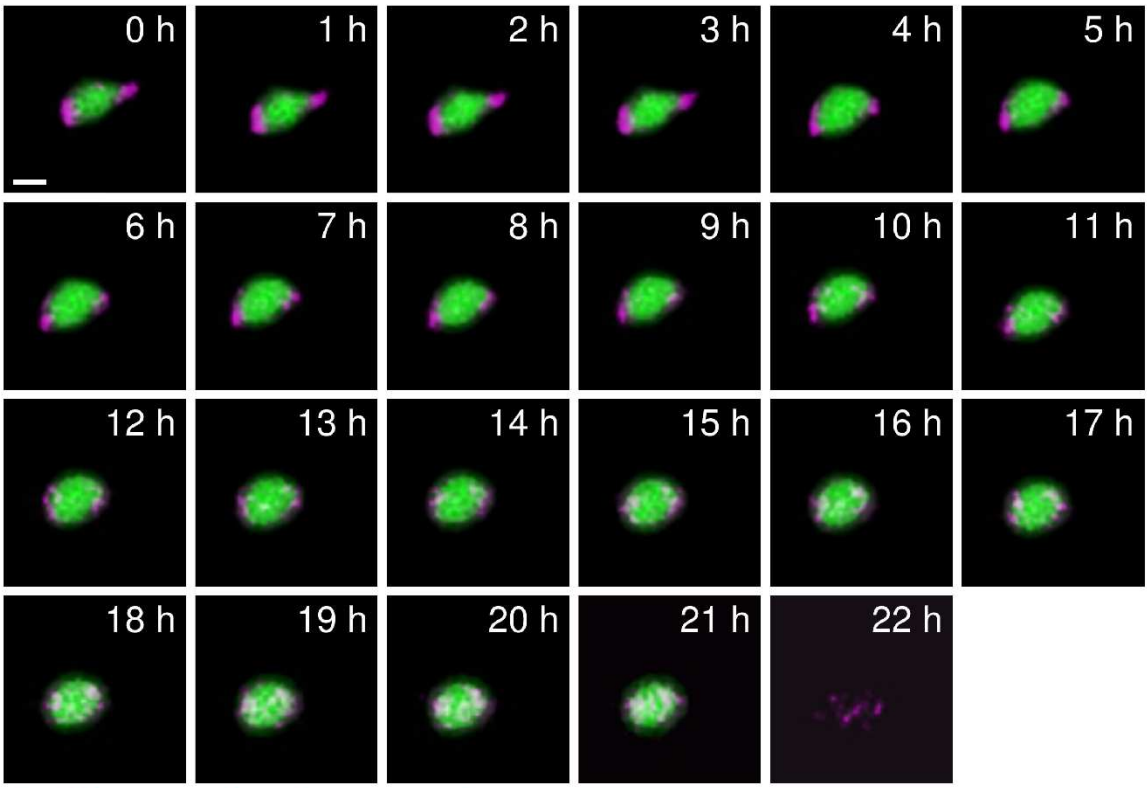

Ca. Nha. antarcticus *Hrr. lacusprofundi*

b

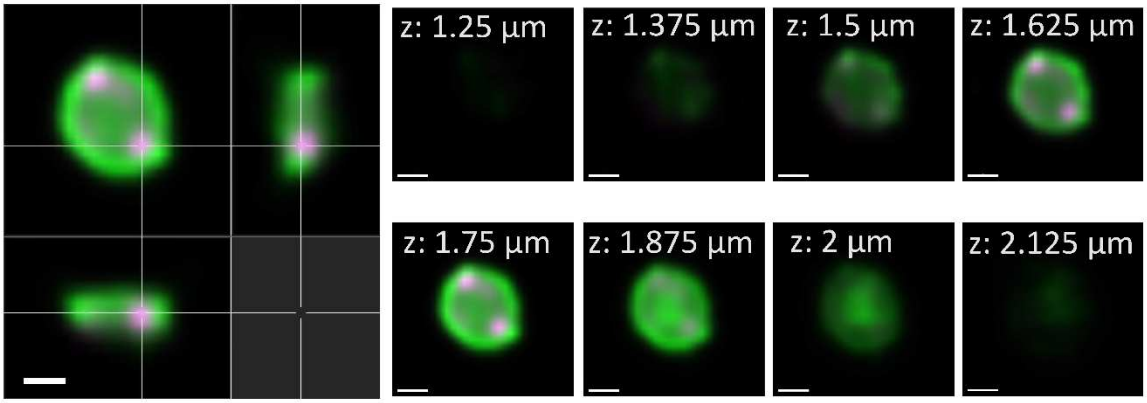

Ca. Nha. antarcticus *Hrr. lacusprofundi*

c

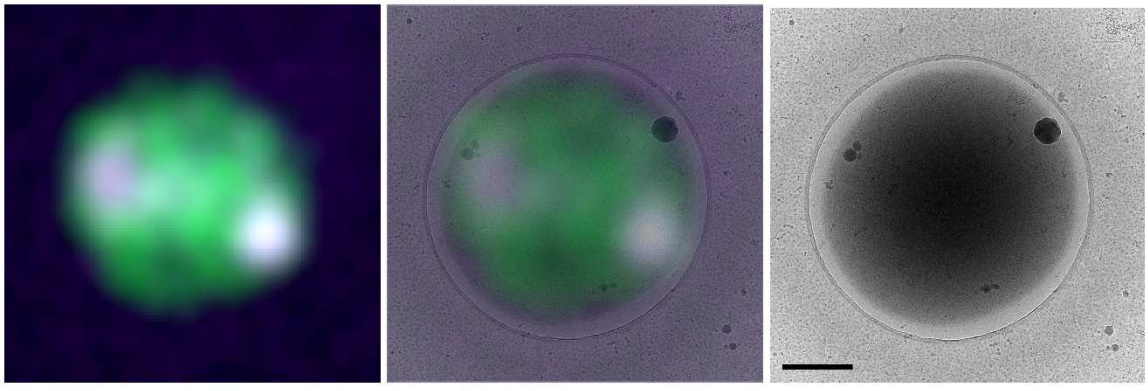

Ca. Nha. antarcticus *Hrr. lacusprofundi*

Fig. 1. Live fluorescence demonstrates *Ca.* Nha. antarcticus enters *Hrr. lacusprofundi* cells. a, Representative live fluorescence time lapse series of *Ca.* Nha. antarcticus cells (MitoTracker DeepRed, coloured Magenta) attached to a host *Hrr. lacusprofundi* cell (MitoTracker Orange, coloured Green) (0 – 9 h), migrating internally (~10 – 21 h), followed by lysis of the host (22 h). **b**, Confocal 3D-orthogonal slice maximum intensity projection showing representative images of *Ca.* Nha. antarcticus cells internalised within *Hrr. lacusprofundi* after 10 h incubation. **c,** Cryo-CLEM of internalised *Ca.* Nha. antarcticus cells (stained with MitoTracker DeepRed, represented Magenta) within a *Hrr. lacusprofundi* cell (stained with MitoTracker Orange, represented Green). Overlay of fluorescence and cryo-TEM data shows the host cell remains intact following internalisation and no sign of the *Ca.* Nha. antarcticus cells on the exterior of the *Hrr. lacusprofundi* cell. Scale bars: **a** – 1 µm, **b** and **c** – 500 nm.

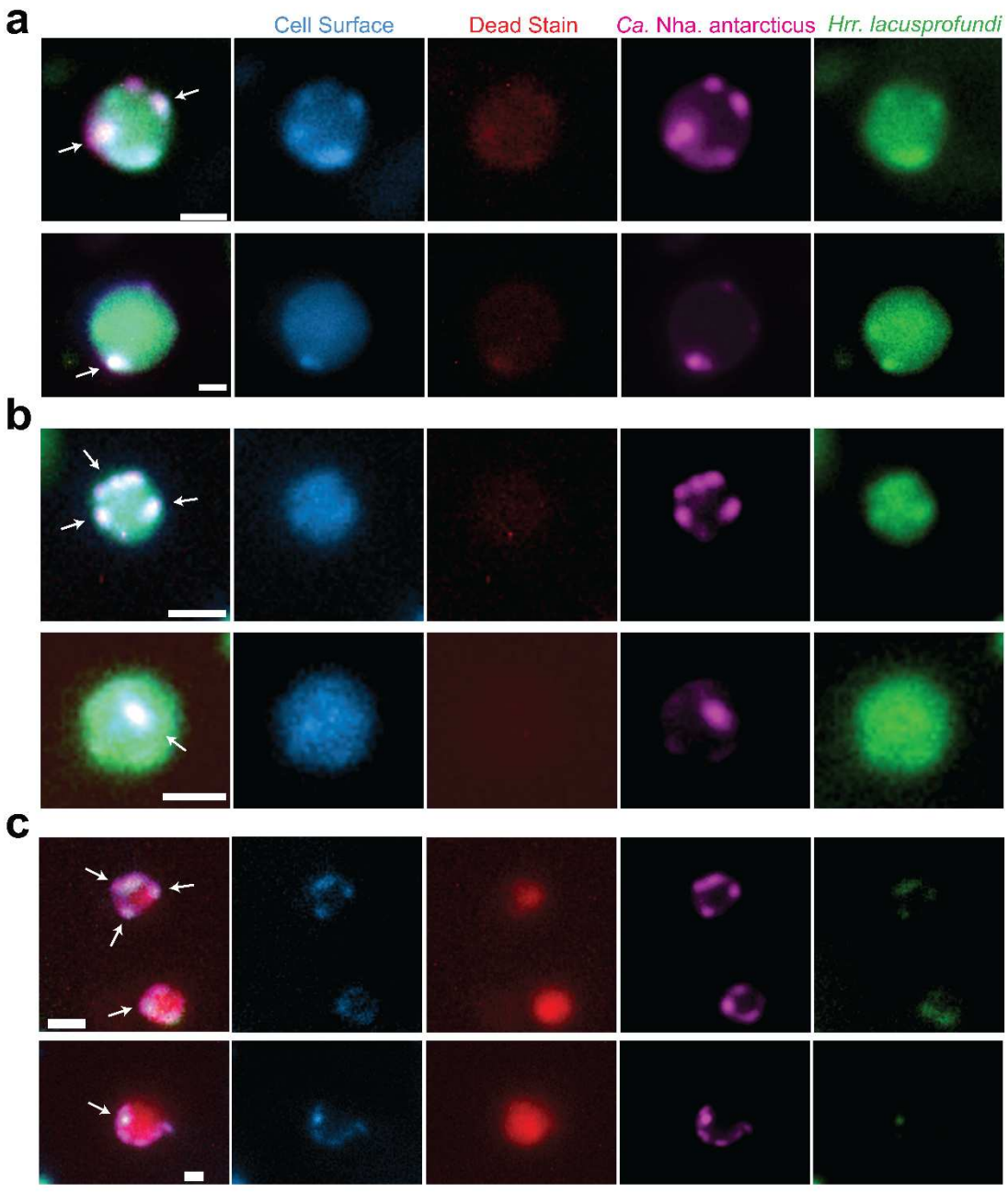

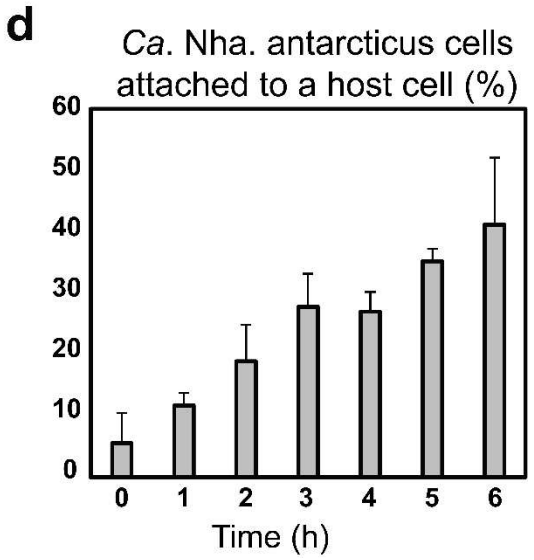

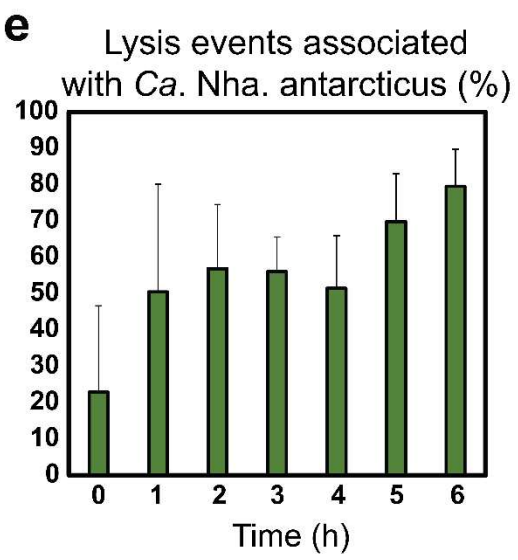

Fig. 2. Fluorescence microscopy of *Ca.* Nha. antarcticus induced cell lysis. a - c Live fluorescence micrographs taken 6 h post-mixing showing *Ca.* Nha. antarcticus (MitoTracker Green, coloured Magenta) interactions with *Hrr. lacusprofundi* (MitoTracker Orange, coloured Green) including additional stains for cell surface (ConA-AF350, coloured Blue), and cell death (RedDot 2, coloured red). **a,** Representative fluorescence micrographs showing *Ca.* Nha. antarcticus cells (MitoTracker Green, coloured Magenta) attached to the surface of *Hrr. lacusprofundi* (MitoTracker Orange, coloured Green). Cell surface staining (ConA-AF350, coloured Blue) shows foci corresponding to regions where *Ca.* Nha. antarcticus was attached to the host cell. No signs of lysis were detected by a dead cell stain (RedDot 2, coloured Red). **b,** Representative live fluorescence micrographs showing *Ca.* Nha. antarcticus cells (stained with MitoTracker Green, represented Magenta) internalised within *Hrr. lacusprofundi* cells (stained with MitoTracker Orange, represented Green). Cell surface staining (Concanavalin A, represented Blue) does not show foci corresponding to *Ca.* Nha. antarcticus cells, indicating the symbiont has become internalised. No signs of lysis are evident from inclusion of a dead stain (RedDot 2, represented Red). **c,** Representative fluorescence of *Hrr. lacusprofundi* (MitoTracker Orange, coloured Green) lysis events associated with *Ca.* Nha. antarcticus (MitoTracker Green, coloured Magenta). Lysis is indicated by positive fluorescence for RedDot 2 (coloured Red) and is associated with loss of MitoTracker Orange signal from the host cell while the *Ca.* Nha. antarcticus cells remain intact and positive for both MitoTracker Green and the cell surface stain (Con-AF350A, coloured Blue). **d,** Quantitative data for lysis and attachment events over short-term incubations. Data show percentage of lysis events associated with a *Ca.* Nha. antarcticus cell and the percentage of *Ca.* Nha. antarcticus cells attached to host cells over the course of a time series (0 – 6 h). Data show average number of events across triplicate experiments, and error bars represent standard deviation as summarised in Table S2. Arrows: examples of *Ca.* Nha. antarcticus cells; Scale bars: 500 nm.

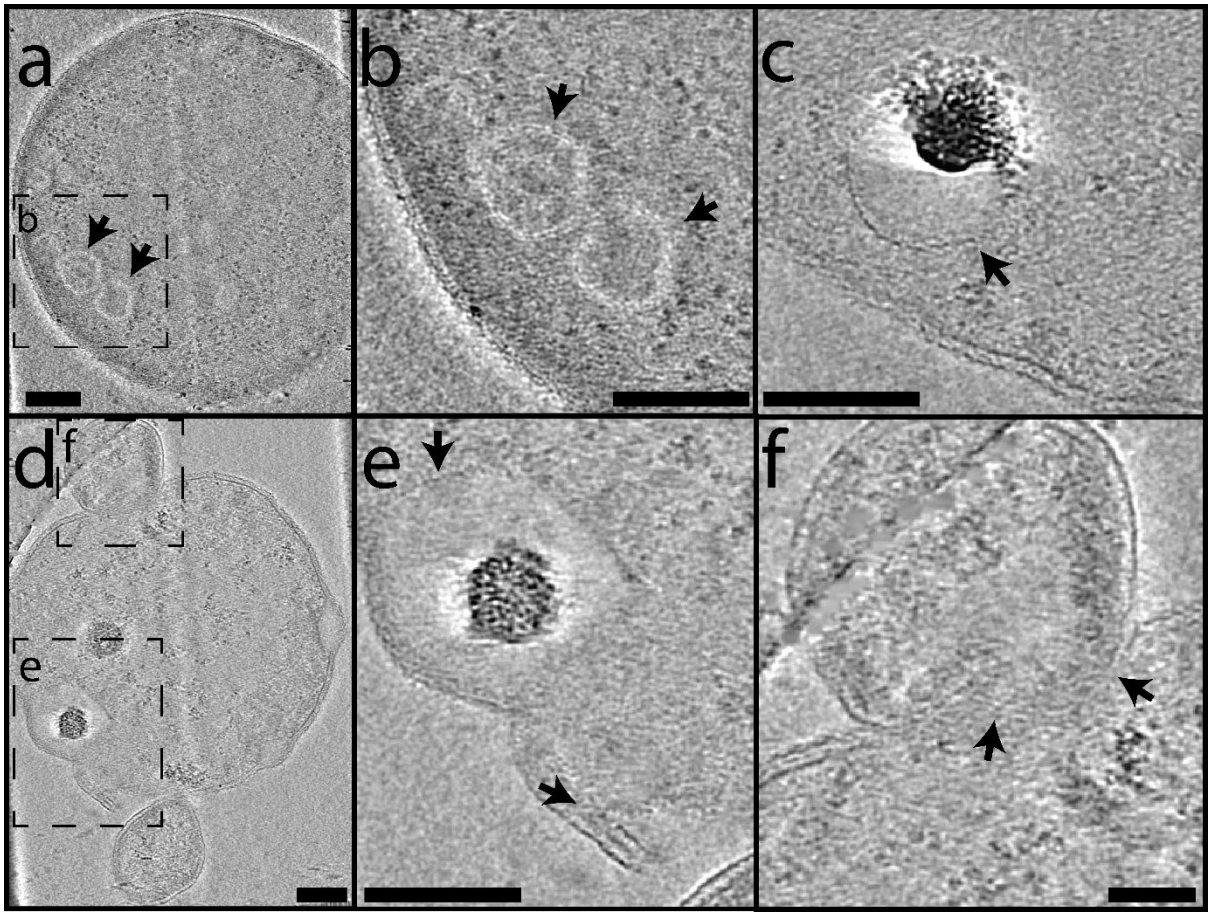

Fig. 3. Cryo-electron tomography of *Ca.* Nha. antarcticus – *Hrr. lacusprofundi* co-cultures show internal membrane bound structures. a – **f**, Z-slices from tomograms (**a** and **b:** Supplementary Video 2, **c:** Supplementary Video 3, **d** - **f:** Supplementary Video 4) showing (**a** – **d**) internal membrane bound structures within *Hrr. lacusprofundi* cells consistent with *Ca.* Nha. antarcticus that have internalised. **a – b,** A *Hrr. lacusprofundi* cell with an intact cell membrane and multiple internal membrane bound structures (arrows). **c,** A *Hrr. lacusprofundi* cell with an intact cell membrane and an internal membrane bound structure (arrow). (**d** – **f**) A *Hrr. lacusprofundi* cell with internal structures consistent with internalised *Ca*. Nha. antarcticus cells (**e**, arrows) and a *Ca*. Nha. antarcticus cell that appears to be in the process of internalising (**f**, arrows indicate region where *Ca.* Nha. antarcticus cell appears to be partially within the *Hrr. lacusprofundi* cell). Images acquired using a Titan Krios at 300 kV. Scale bars: 100 nm

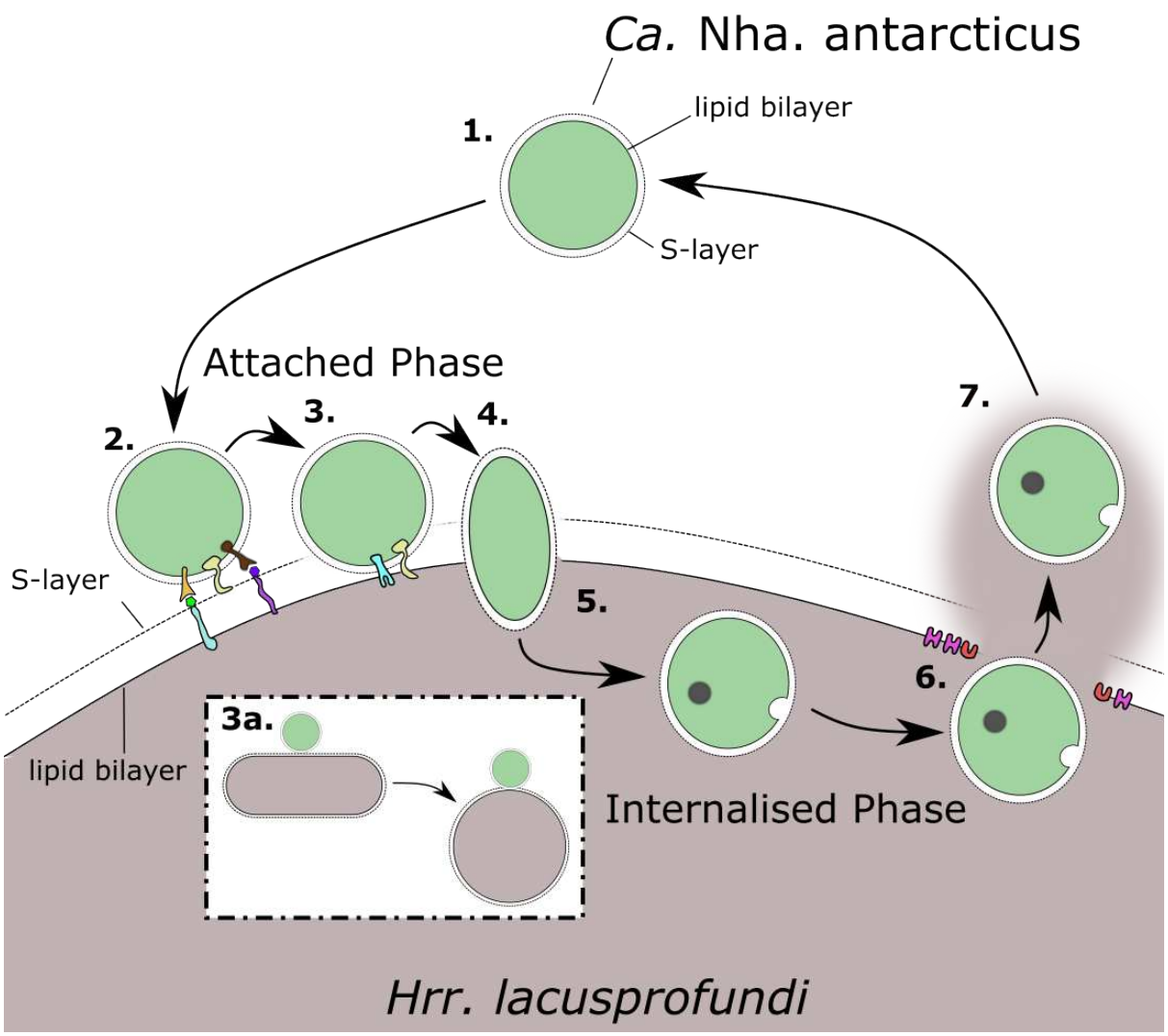

Fig. 4. Proposed lifestyle of *Ca.* Nha. antarcticus. 1) Unattached Stage: *Ca.* Nha. antarcticus cells utilise nutrient stores accumulated during interactions with *Hrr. lacusprofundi* to enable survival until a new host cell is encountered and successfully invaded. **2)** Host Recognition Stage: Initial attachment involves host recognition and adhesion potentially mediated by *Ca.* Nha. antarcticus proteins with domains including cell adhesion domains including Ig-folds (e.g. SPEARE protein[8]; yellow), lectin/glucanase domains (brown), and pectin lyase domains (orange), which likely bind to sugar moieties on host glycolipids and glycoproteins. **3)** Pre-Invasion Stage: Localised degradation of the host S-layer by proteases including potentially the protease domain on the SPEARE protein (yellow) enables *Ca.* Nha. antarcticus access to the *Hrr. lacusprofundi* membrane. **3a)** The localised degradation of the host S-layer can destabilise host cell morphology and cause some rod-shaped

host cells to become coccoidal. The timing of morphological change varies and is likely dependent on a range of factors such as the site of invasion and size of the cells. **4)** Invasion Stage: The *Ca.* Nha. antarcticus cell passes into the host cell; pore-forming proteins such as the *Ca.* Nha. antarcticus SPEARE protein may function in this stage. **5)** Internalised Stage: while internalised, *Ca.* Nha. antarcticus cells acquire nutrients from *Hrr. lacusprofundi* for proliferation and generate stores of nutrients including PHA-like granules (grey) and membrane embedded lipid droplets. **6)** Host Lysis Stage: The *Hrr. lacusprofundi* membrane is destabilised and many host cells lyse. **7)** Release Stage: *Ca.* Nha. antarcticus cells are released into the environment, enabling them to re-enter the Unattached Stage.

Supplementary Materials:

Figs. S1 – S17

Tables S1 and S2

Supplementary Videos 1 – 15